**POAC'13**
Espoo, Finland

Proceedings of the 22nd International Conference on
**Port and Ocean Engineering under Arctic Conditions**
**June 9-13, 2013**
**Espoo, Finland**

POAC13-022

# A Reliability-Based Approach to Determine Local Ice Design Pressures

Guang (George) Li

Shell International Exploration and Production

Houston, TX, USA

## ABSTRACT

Design values of local ice pressure may govern the member sizing of an arctic structure that is subject to ice actions. Although the local pressure-area relationships are provided in some design codes (e.g. ISO 19906:2012), questions remain on how to apply such a relationship to a structural design process, which often utilizes finite element method.

In this paper, a structural reliability-based approach is proposed to define the design local pressure distributions associated with the structural members under design. The local pressures are treated as random processes with pre-defined correlation functions. These random processes are transferred to a new set of independent processes to enable the Monte Carlo simulations (MCS). The First-Order Reliability Method (FORM) and Second-Order Reliability Method (SORM) can then be applied to define the design pressure distributions. Finally, this new approach is illustrated in an example using beam finite element.

## INTRODUCTION

Design values of local ice pressure may govern the member sizing of an arctic structure that is subject to ice actions. As a result, they often drive the weight of the primary steel or outer shell of the structure, and its fabrication/installation costs.

In order to obtain realistic values of local ice pressure representative of the field conditions, researchers in the past (e.g., Iyer and Masterson, 1987; Masterson et al., 1992) used indenters in the field to measure the local pressure in highly confined conditions. Masterson and Frederking (1993) compiled the results from the indentation tests and from ship trials. They observed an inverse relationship between area ($A$) and local pressure ($p$). They proposed the following formula as an upper bound of the field data:

$$p = \begin{cases} 8.1A^{-0.5} & 0.1 < A < 29m^2 \\ 1.5\ MPa & A \geq 29m^2 \end{cases} \quad (1)$$

This pressure-area relationship was adopted in the CSA S-471 code on loadings on offshore structures and in the API PR2N offshore structure code.

Recently, Masterson et al. (2007) revised the CSA S-471 pressure-area relationship by excluding ship impact tests and including additional data from the Molikpaq measurements in the Beaufort Sea. They proposed the following formula as an upper bound of the field data:

$$p = \begin{cases} 7.4A^{-0.7} & A \le 10m^2 \\ 1.48\ MPa & A > 10m^2 \end{cases} \quad (2)$$

This revised pressure-area relationship was adopted for thick, massive ice features in the new ISO 19906:2010(E) code for arctic offshore structures. Interestingly, the ISO pressure-area relationship is *three* times standard deviation from the mean values while the CSA relationship is *two* times standard deviation from the mean values although the ISO relationship yields lower pressure for areas larger than 0.65 $m^2$. This inconsistency reflects the importance of the data selection for the statistical analysis.

ISO 19906 provides the following requirements on contact area considerations in Subsection 8.2.5:

> "Design contact areas shall be considered based on the local structural configuration, including frame spacing, plate thickness and appendage dimensions. The size and placement of the local contact areas shall be selected to ensure that the most critical cases are addressed.
>
> Local ice actions shall be considered in the context of background actions on adjacent panels or areas of the structure."

However, there is no guidance in ISO 19906 on how to select the most critical cases of the size and placement of the local contact areas. It is also unclear what pressure values should be chosen on the adjacent panels or areas. Structure designers face the dilemma of having to come up with a scantling design (frame spacing, plate thickness, etc.) against potentially infinite number of pressure and area combinations.

ISO 19906 also permits probabilistic local design for thick, massive ice features based on data from ship impacts with multi-year ice floes (Jordaan et al., 1993). The probability distribution of the local peak pressure can be modelled as a function of exposure and contact area. Brown (1996) used such an approach to optimize the bow plating by considering the uncertainties in local ice pressure (treated as a single random variable) and structural properties. However, a designer still faces the issue of choosing the most critical cases of the size and placement of the local contact areas.

In order to close this gap between ice engineering and structural engineering, a structural reliability-based approach is proposed in this paper. A framework to evaluate the reliabilities of structural members under local ice actions is presented next. Then, a simple example using beam finite element is provided as an illustration of this framework. Finally, remaining works for future improvements are discussed.

## A RELIABILITY-BASED FRAMEWORK

An offshore structure located in the arctic may be subject to multiple ice interactions each year. In each loading event, the local pressure for a given area is stochastic in nature and varies as a function of time, i.e. a random process. For any given time, the pressure for the given area can be modelled as a random variable and the pressures for the given area and its surrounding areas can be modelled as a random field. This idea is illustrated in Figure 1 where Zone 1 is the given area.

| | | |
|---|---|---|
| Zone 9 | Zone 2 | Zone 3 |
| Zone 8 | Zone 1 | Zone 4 |
| Zone 7 | Zone 6 | Zone 5 |

*Figure 1* Pressure Zones

A statistical model can be used to describe the random pressure field with the pressure-area relationship implicitly built into this statistical model. For example, Spencer and Morrison (2012) proposed a statistical model that can reproduce the ISO formulation of *global* ice pressure as a function of structure width and ice thickness. For the panel size of 0.5m x 0.5m, they modelled the pressure variable with a mean of 0.85 MPa and a standard deviation of 2 MPa. Pressures of adjacent and non-adjacent panels were modelled with a correlation function following the power law.

To generalize, a vector $\mathbf{P} = [\mathrm{P}_1 \quad \mathrm{P}_2 \quad \cdots \quad \mathrm{P}_n \,]^{\mathrm{T}}$ is used to represent the ice pressures in n zones of interest. The pressure in each zone is modelled as a stationary random process with its mean and standard deviation. If we subtract its mean value from each pressure process and then normalize it against its standard deviation, we can obtain a new zero-mean, unit-variance vector $\boldsymbol{X}$; i.e.

$$\boldsymbol{X} = \left[\frac{\mathrm{P}_1-\mathrm{m}_1}{\sigma_1} \quad \cdots \quad \frac{\mathrm{P}_n-\mathrm{m}_n}{\sigma_n}\right]^{\mathrm{T}} = \boldsymbol{\sigma}^{-1}\,(\boldsymbol{P}-\boldsymbol{m}) \tag{3}$$

Where $\boldsymbol{m}$ is the mean vector and $\boldsymbol{\sigma}$ is a sparse matrix with all its non-zero elements of $\sigma_1 \quad \cdots \quad \sigma_n$ in its main diagonal.

The correlation matrix of $\boldsymbol{X}$ is the same as the one of $\boldsymbol{P}$ and is defined as the following:

$$\boldsymbol{c_X} \equiv \mathrm{E}[\boldsymbol{X}\,\boldsymbol{X}^{\mathrm{T}}] = \begin{bmatrix} 1 & \cdots & \mathrm{c}_{1n} \\ \vdots & \ddots & \vdots \\ \mathrm{c}_{n1} & \cdots & 1 \end{bmatrix} \tag{4}$$

The means and standard deviations of local ice pressure, as well as the correlation matrix $\boldsymbol{c_X}$, are obtained by analyses of field or test data. For example, Taylor (2010) calculated the correlation coefficients of ice pressures (shown in Figure 2) based on JOIA data.

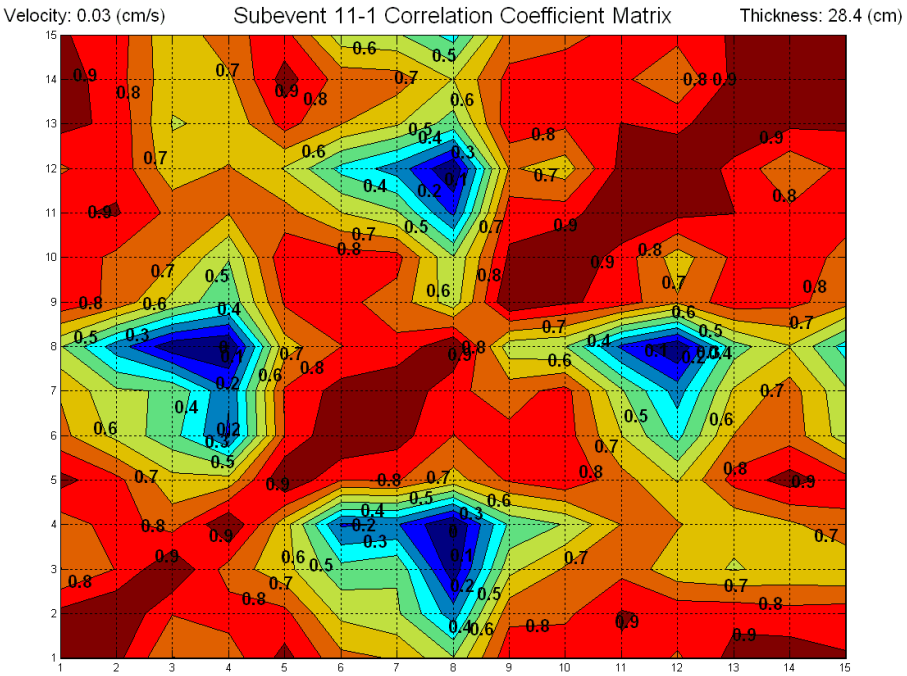


*Figure 2* Correlation coefficient matrix contour plot (Taylor, 2010)

***Monte Carlo Simulation (MCS) Approach***

In theory, a structural analyst can simulate the correlated local pressure field as functions of time, and then apply the time histories of the ice pressure to the structural model to obtain the structural responses. Through MCS, the analyst can then calculate the reliability of the given structural design. As discussed earlier, the statistical model describing the pressure field ensures that the pressure-area relationship is satisfied implicitly. The load panel size can be reduced iteratively until the calculated reliability values converge.

In order to simulate the *correlated* pressure field, a vector of zero-mean, unit-variance vector *independent* random processes is simulated first. This vector, denoted as $\boldsymbol{U}$**,** is transformed into the vector $\boldsymbol{X}$ by the following equation

$$\boldsymbol{X} = \boldsymbol{b}\,\boldsymbol{U} \tag{5}$$

where $\boldsymbol{b}$ is the transformation matrix.

Plugging Eq. 5 into Eq. 4 one obtains the following:

$$\boldsymbol{c_X} \equiv E[\boldsymbol{b}\,\boldsymbol{U}\,\boldsymbol{U}^T\boldsymbol{b}^T] = \boldsymbol{b}\,\boldsymbol{b}^T \tag{6}$$

There are many possible solutions of the transformation matrix $\boldsymbol{b}$ based on the equation above. In order to facilitate the solution, the transformation matrix $\boldsymbol{b}$ is limited to the following structure

$$\boldsymbol{b} = \begin{bmatrix} b_{11} & 0 & 0 & \cdots & 0 \\ b_{21} & b_{22} & 0 & \ldots & 0 \\ b_{31} & b_{32} & b_{33} & \ddots & \vdots \\ \vdots & \vdots & \vdots & \ddots & 0 \\ b_{n1} & b_{n2} & b_{n3} & \cdots & b_{nn} \end{bmatrix} \tag{7}$$

Eq. 6 can then be solved by solving each element in the transformation matrix $\boldsymbol{b}$ from top to bottom and from right to left in the sequence of $b_{11} \rightarrow b_{21} \rightarrow b_{22} \rightarrow b_{31}$ ...

***Structural Reliability Approach***

If the finite element method (FEM) is used for structural design, the MCS approach outlined previously will require a large computational effort and may become impractical due to time and resource constraints. Therefore, we examine some special cases where there are numerically efficient approaches.

If the pressure vector $\boldsymbol{P}$ is Gaussian, then the zero-mean, unit-variance vector $\boldsymbol{U}$ is also Gaussian. For this special case and the case of independent pressure vector $\boldsymbol{P}$, the FORM (first-order reliability method) and SORM (second-order reliability method) approaches (Ditlevsen and Madsen, 1996) can be easily applied and are very numerically efficient. The limit state function is numerically defined by the FE model for the structural design.

Application of the FORM or SORM numerically will yield a design point $\boldsymbol{u_0}$, a reliability index $\beta$ and a unit vector $\boldsymbol{\alpha}$. The design point $\boldsymbol{u_0}$ is the closest point to the origin on the limit state surface in the $\boldsymbol{U}$ space, and the reliability index $\beta$ is the distance from the origin to the design point. Physically, the design point represents the pressure combination that is the most likely to reach the limit of the structural capacity. The unit vector $\boldsymbol{\alpha}$ points towards the design point from the origin. Projection of the vector $\boldsymbol{U}$ onto the unit vector $\boldsymbol{\alpha}$ yields a new random process, denoted as reliability-weighted normalized pressure $\hat{P}$, i.e.

$$\hat{P} = \boldsymbol{\alpha}^T\,\boldsymbol{U} \tag{8}$$

If at any time instance the value of $\hat{P}$ is equal or greater than the reliability index $\beta$, the structural capacity is then reached or exceeded. The probability of the reliability-weighted

normalized pressure $\hat{P}$ staying less than the reliability index $\beta$ represents the structural reliability in a given ice-interaction event.

## NUMERICAL EXAMPLE

To illustrate this reliability-based framework, a simple beam finite element problem is solved here as an example.

For simplicity, it is assumed the pressure vector $\boldsymbol{P}$ is independent, i.e. zero-correlations. Based on the statistical averaging method (Jordaan et al., 2006), the standard deviation of the pressure on a given area $A$ is then given as (after Spencer and Morrison, 2012)

$$\sigma(A) = \sigma(A_0)\left(\frac{A}{A_0}\right)^{-0.5} \tag{9}$$

where $A_0$ is the area of the reference panel.

Using the values given in Table 1, the pressure-area curve three times standard deviation from the mean values gives a reasonably good upper bound to the field data as shown in Figure 3; i.e., the pressure-area relationship is implicitly satisfied using this simple correlation model.

Table 1. Pressure Statistics of Reference Panel.

| $A_0$, m$^2$ | Mean Pressure, MPa | $\sigma(A_0)$, MPa |
|---|---|---|
| 0.15 | 1 | 6.27 |

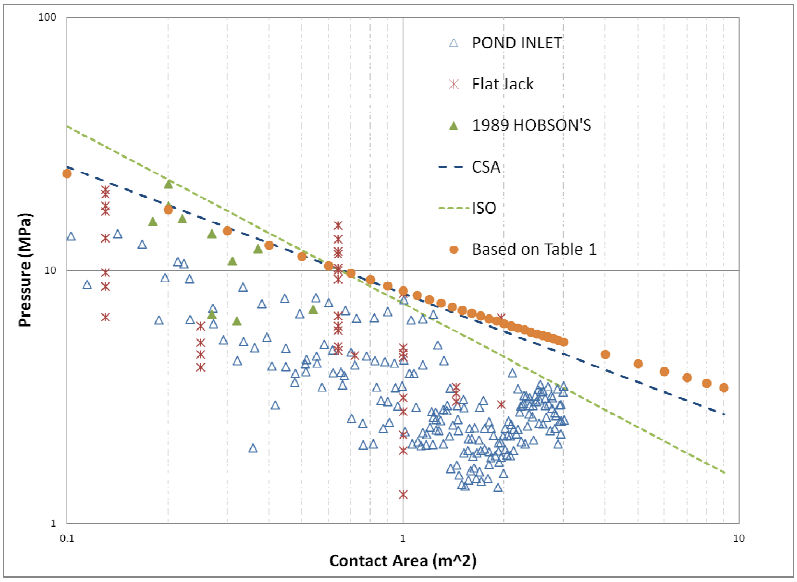


*Figure 3* Upper Bounds of Pressure Data

The reliability of a beam *clamped* at both ends supporting a panel (Figure 4) is investigated in this example. This is analogous to a stringer in a continuous stiffened plate. The properties of the structural members are listed in Table 2. The panel area is divided into multiple strips equally (Figure 4) and the average pressure in each strip is a treated as a random process with its statistical properties obtained following Eq. 9 and Table 1.

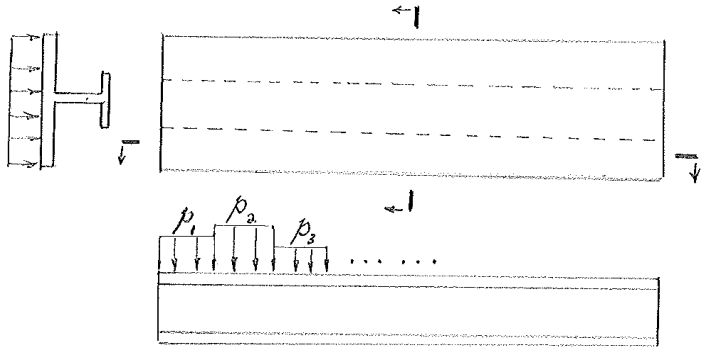

*Figure 4* A Beam Subject to Local Ice Pressure

Table 2. Properties of the Beam and Panel

| | |
|---|---|
| Length of the beam | 3 m |
| Width of the panel | 0.8 m |
| Bending stiffness (EI) | 3.6E08 N-m^2 |
| Moment of yield | 6.0E06 N-m |

First, the limit state is defined as the average of the moments at *both* ends of the beam reaches the elastic limit. For the case where the panel is divided into 12 load strips, FEA yields the following relationship between the average moment and the pressure vector

$$\bar{M} = \{0.015 \quad 0.041 \quad 0.061 \quad 0.077 \quad 0.088 \quad 0.093 \quad \text{symmetric}\}\ P \qquad (10)$$

The reliability index is found to be 5.27 and its corresponding probability of exceedance at any time instance is 6.8E-08. The panel is also divided into 2, 4, and 24 strips to investigate convergence (Figure 5). Note that the standard deviation of the pressure in each strip increases when the strip area decreases (Eq. 9).

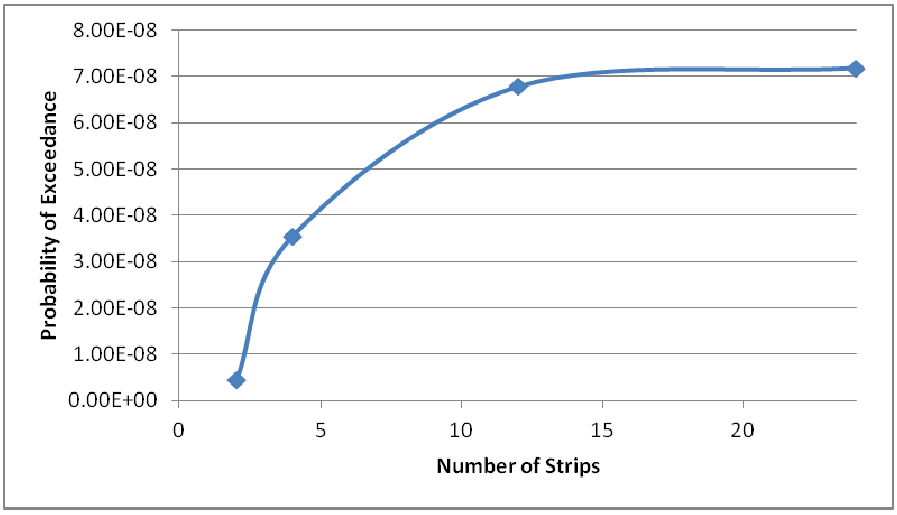


*Figure 5* Convergence of Probability of Exceedance

Figure 5 shows that convergence has been achieved with 24 load strips. Also, insufficient number of strips (e.g. 2 or 4) can lead to significant underestimate of the probability of exceedance by as much as a factor of ten. In other words, assuming a uniform pressure across the beam panel is non-conservative.

The design pressure distribution (i.e. the most likely distribution to reach the limit of the structure capacity) is shown in Figure 6 on half of the beam (due to symmetry) for different number of strips. The pressure in each strip is plotted at the centre of the strip. Figure 6 shows that the pressure distribution has also reached convergence with 24 load strips.

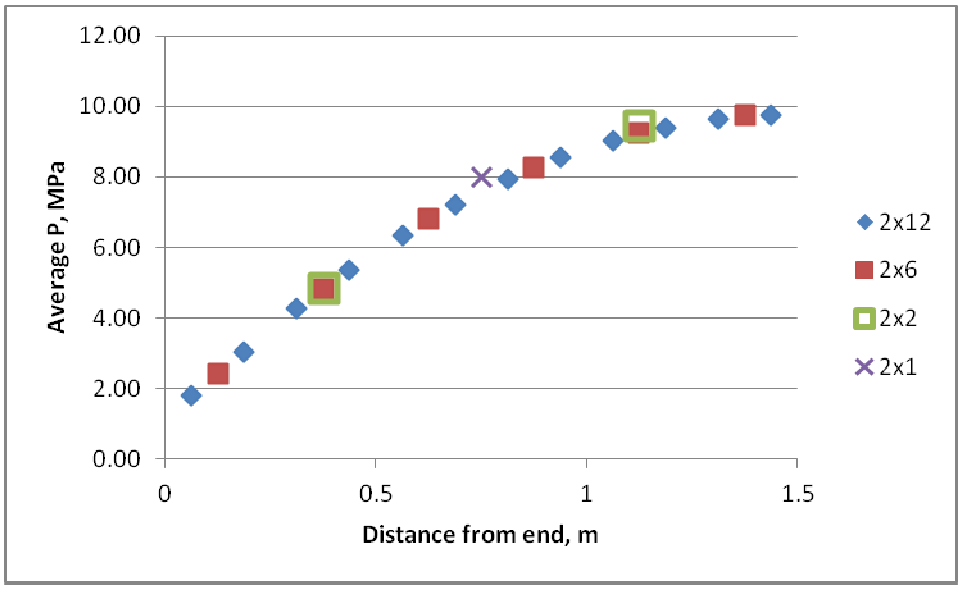


*Figure 6* Design Pressure Distribution on Half of the Beam

The unit reliability vector $\boldsymbol{\alpha}$ for 12 strips is solved as following

$$\boldsymbol{\alpha} = \{0.064 \quad 0.172 \quad 0.260 \quad 0.327 \quad 0.371 \quad 0.393 \quad symmetric\}^T$$

The peaks of the reliability-weighted normalized pressure $\hat{P}$ (defined by Eq. 8) follow a Rayleigh distribution if it is narrow-banded (Bendat and Piersol, 2000). The following characteristics of the crushing process are assumed based on works by Karna et al. (2006): zero up-crossing frequency of 0.7 Hz, ice velocity of 0.15 m/s, and a penetration length of 300 m. The probability of the beam reaching its limit under such a loading event is calculated to be 1.3E-03.

If the limit state is defined differently as the moment at the near end of the beam reaching its elastic limit, then the solutions are also different. For 12 load strips (sufficient number of strips as shown in Figure 5), the reliability index is found to be 5.05 and its corresponding probability of exceedance at any time instance is 2.93E-07. Figure 7 shows the probabilities for different number of strips. The probability of exceedance for this limit state of yielding at the near end of beam is significantly higher than that of the limit state of yielding at *both* ends because the latter is a more stringent requirement. This difference shows the importance of selecting the appropriate limit state for design.

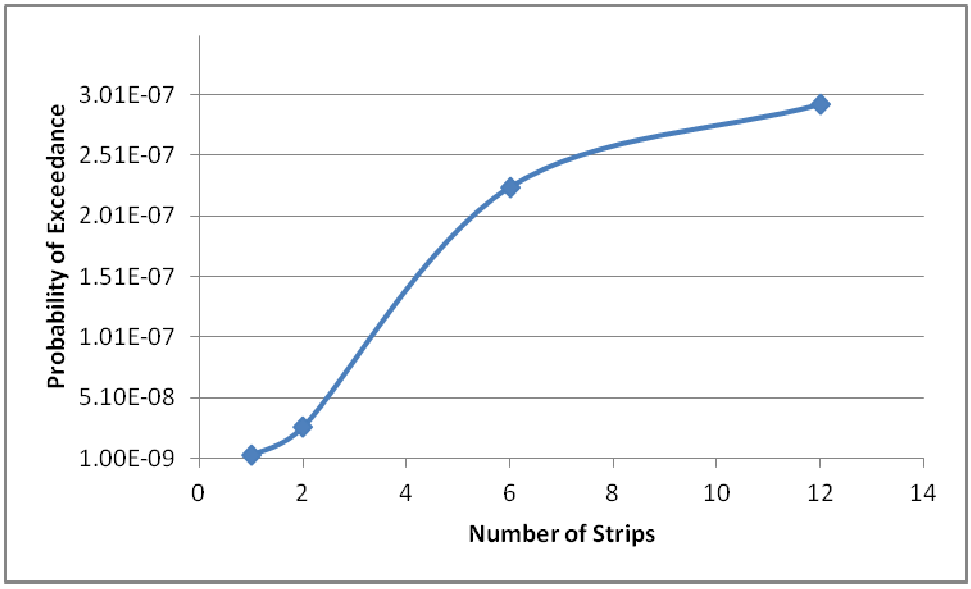


*Figure 7* Probability of Exceedance for Near End to Yield

The design pressure distribution (i.e. the most likely distribution to reach the limit of the structure capacity) is shown in Figure 8 for difference number of strips. As expected, the pressure distribution is unsymmetrical and the high pressure zones (i.e. the critical placement) are closer to the near end of the beam, where yielding defines the structural limit state.

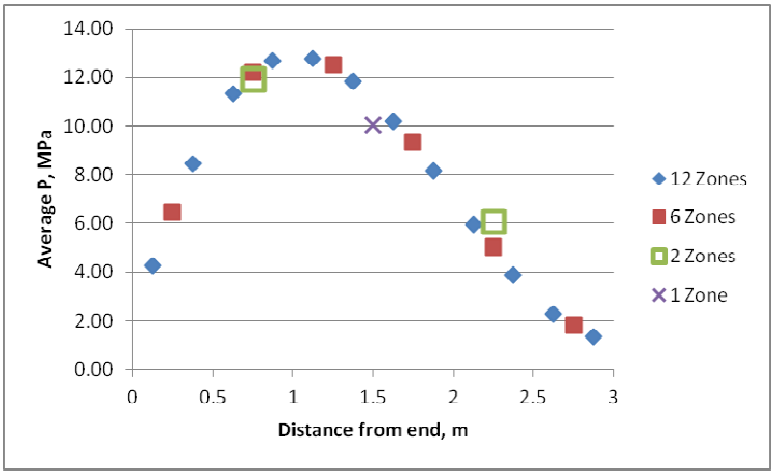


*Figure 8* Design Pressure Distribution for Near End to Yield

The unit reliability vector $\boldsymbol{\alpha}$ for 12 strips is solved as following

$$\boldsymbol{\alpha} = \{0.12 \quad 0.27 \quad 0.38 \quad 0.43 \quad 0.43 \quad 0.4 \quad 0.34 \quad 0.26 \quad 0.18 \quad 0.11 \quad 0.05 \quad 0.01\}^T$$

Based on the previous assumptions of the reliability-weighted normalized pressure (defined by Eq. 8), the probability of reaching the elastic limit at the near end of the beam is calculated to be 4.1E-03 in the same loading event as discussed previously. Using simple probability theory, the probability of reaching the elastic limit at *either* end of the beam is calculated to be 6.9E-03 in the same loading event.

## DISCUSSIONS AND CONCLUSIONS

A structural reliability framework is proposed in this paper to assess the reliabilities of structural members under local ice load. The random pressure field can be statistically characterized to implicitly account for the pressure-area relationship. Then, MCS technique

can be used (at least in theory) to assess the structural reliability. For special cases of uncorrelated pressures between load zones and of Gaussian pressure processes, numerically efficient reliability methods (FORM and SORM) can be used for the assessment. The concept of reliability-weighted normalized pressure is proposed to account for the time-varying nature of the pressure field.

The earlier example shows that insufficient number of load zones can significantly underestimate the failure probability since the design pressure distribution cannot be adequately captured by insufficient number of load panels. On the other hand, the structural reliability assessment converges with sufficient number of load panels. Also, the design pressure distribution depends on the selected limit state of the structure.

In order to adopt the proposed framework to guide structural design, the following items should be addressed.

1. An effective statistical representation of the random ice pressure field needs to be developed. Correlations between different pressure zones should be investigated. As shown in Figure 3, assumption of independence yields an exponent of -0.5 in the pressure-area relationship, which is likely conservative for design.
2. Statistical distribution of the underlying pressure processes need to be investigated. Distributions, besides Gaussian, may be used due to the unsymmetrical nature of the processes with respect to their mean values.
3. Other statistical properties of the pressure processes, e.g. bandwidth, number of peaks, and peak distributions, need to be analyzed. Jordaan (1993) proposed exponential or Gumbel distributions for the pressure peaks depending on the loading duration. The peak distribution needs to be consistent with the underlying processes in order to adopt this reliability framework.
4. The structural reliability and design pressure distribution depend on the selected limit state of the structure. Elastic limit states may be too conservative and costly given the large surface area of a GBS in the arctic. Some yielding should be allowed if the structural material is ductile.
5. For simplicity, the earlier example did not consider the uncertainties associated with the structure member, e.g. dimensions and mechanical properties. Future work should include these uncertainties to assess the structural reliability properly and to optimize the structure design (Brown, 1996). The proposed framework can be used to calibrate load and resistance factors for LRFD approach.

## ACKNOWLEDGEMENT

The author would like to thank Shell International Exploration and Production Company for funding this study and for permission to publish. He also thanks Dr. Rocky Taylor and Dr. Ian Jordaan for providing a copy of Figure 2 and Dr. Robert Frederking for sharing the underlying data of Figure 3 and providing helpful comments to improve this paper.

## REFERENCES

Bendat, J.S. and Piersol, A.G. Random Data: Analysis and Measurement Procedures (3rd Edition). John Wiley & Sons, 2000.

Brown, P.W. et al., 1996. Optimization of Bow Plating for Icebreakers. Journal of Ship Research, 50, pp. 70 – 78.

Ditlevsen, O. and Madsen, H.O., 1996. Structural Reliability Methods. John Wiley & Sons, June 1996.

ISO (International Standards Organization), 2010. Petroleum and Natural Gas Industries – Arctic Offshore Structures, ISO 19906:2010(E).

Iyer, S.H. and Masterson, D.M., 1987. Field Strength of Multi-Year Ice Using Thin-Walled Flat Jacks. Proceedings of the 9th International Conference on Port and Ocean Engineering under Arctic Conditions (POAC), Fairbanks, USA.

Jordaan, I.J. et al., 1993. Probabilistic Analysis of Local Ice Pressures. Journal of Offshore Mechanics & Arctic Engineering, 115, pp. 83 – 89.

Jordaan I.J., Frederking R., Li C., (2006) Mechanics of Ice Compressive Failure, Probabilistic Averaging and Design Load Estimation. Proceedings of the 18th International Ice Symposium (IAHR), Sapporo, Japan

Karna, T. et al., 2006. An Extreme Value Analysis of Local Ice Pressures. Proceedings of the 8th International Conference and Exhibition on Performance of Ships and Structures in Ice (ICETECH), Banff, Canada.

Masterson, D.M. et al., 1992. Pressure vs. Area Relationships from Medium Scale Iceberg Impact Test Program. Proceedings of the 11th International Ice Symposium (IAHR), Banff, Canada.

Masterson, D.M. and Frederking, R.M.W., 1993. Local Contact Pressures in Ship/Ice and Structure/Ice Interactions. Journal of Cold Regions Science and Technology, 21, pp. 169 – 185.

Masterson, D.M. et al., 2007. A Revised Ice Pressure-Area Curve. Proceedings of the 19th International Conference on Port and Ocean Engineering under Arctic Conditions (POAC), Dalian, China.

Spencer, P.A. and Morrison, T.B., 2012. High Pressure Zones, Statistics and Pressure-Area Effects. Proceedings of the 10th International Conference and Exhibition on Performance of Ships and Structures in Ice (ICETECH), Banff, Canada.

Taylor, R.S., 2010. Analysis of Scale Effect in Compressive Ice Failure and Implications for Design. Ph.D. Dissertation, Memorial University of Newfoundland, Canada.